Disperse Multiphase Turbulence with OpenFOAM

Gas-particle decoupling in volcanic plumes and density currents

Matteo Cerminara[1] and Tomaso Esposti Ongaro[1]

[1] Istituto Nazionale di Geofisica e Vulcanologia
Sezione di Pisa, Italy

March 27, 2015

Outline

Geophysical phenomenon

Eruption occurred at Sakurajima volcano (South Japan) in 2012

Geophysical phenomenon: Volcanic Ash Plume

- Compressibility
- Momentum and Buoyancy at the vent
- Particle grain size distribution
- Particle settling
- Turbulent entrainment and heating of atmospheric air
- Buoyancy reversal
- Atmospheric stratification
- Turbulent infrasound
- Wind effects

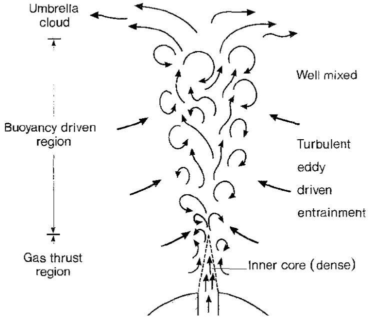

Figure: Volcanic ash plume (Woods, *Bulletin of Volcanology*, 1988).

Motivation

- Large scale: Geophysical phenomena are intrinsically large scale and do not scale to the laboratory scale
- Hazard: Understanding volcanic plumes and pyroclastic density currents is very important for risk assessment
- Real-time monitoring: 3D numerical simulations are a tool to calibrate fast empirical models used for the real-time monitoring of active explosive volcanoes
- Moreover, numerically simulate such a kind of extreme phenomena is an excellent test bench for compressible multiphase CFD solvers

Short term objectives

2-3D models and simulations

- To write a well posed mathematical model based on clear physical assumptions.
- To discretize it implementing a new solver in OpenFOAM – equilibriumEulerianFoam
- To model accurately volcanic ash dynamics, in particular:
  - turbulence
  - preferential concentration (i.e. disequilibrium between the solid and gaseous phase)
- To study the dependence of the plume observables on the input parameters:
  - velocity
  - temperature
  - total ejected mass
  - particle size distribution

Multiphase flow model: main assumptions

- Discrete number of particle classes (polydispersed grain size)

Total grain size of Vesuvius AD 79 (Pompei) eruption ($d = 2^{-\phi}$ mm)

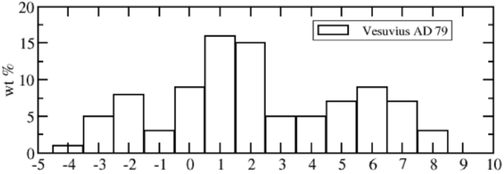

- Heavy particles: $\frac{\hat{\rho}_s}{\hat{\rho}_g} \gg 1$ ($\hat{\rho}_s \approx 400 - 3000$ kg/m^3). Two-way coupling.
- Low concentration $V_s/V := \epsilon_s < 10^{-3}$. Particles are non-interacting (pressureless).
- Large number of particles. Each class can be described as a continuum (Eulerian approach)

All these assumptions are valid for volcanic ash when you are sufficiently higher than the vent and the deposition layer.

Multiphase flow model: main assumptions

- Discrete number of particle classes (polydispersed grain size)

Total grain size of Vesuvius AD 79 (Pompei) eruption ($d = 2^{-\phi}$ mm)

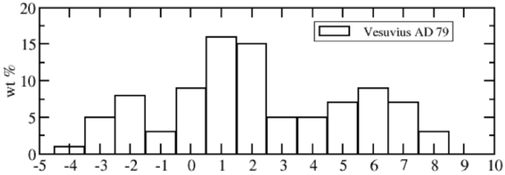

- Heavy particles: $\frac{\hat{\rho}_s}{\hat{\rho}_g} \gg 1$ ($\hat{\rho}_s \approx 400 - 3000$ kg/m^3). Two-way coupling.
- Low concentration $V_s/V := \epsilon_s < 10^{-3}$. Particles are non-interacting (pressureless).
- Large number of particles. Each class can be described as a continuum (Eulerian approach)

All these assumptions are valid for volcanic ash when you are sufficiently higher than the vent and the deposition layer.

Multiphase flow model: main assumptions

- Discrete number of particle classes (polydispersed grain size)

Total grain size of Vesuvius AD 79 (Pompei) eruption ($d = 2^{-\phi}$ mm)

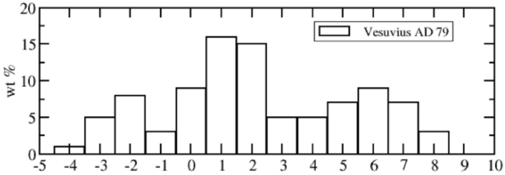

- Heavy particles: $\frac{\hat{\rho}_s}{\hat{\rho}_g} \gg 1$ ($\hat{\rho}_s \approx 400 - 3000$ kg/m^3). Two-way coupling.
- Low concentration $V_s/V := \epsilon_s < 10^{-3}$. Particles are non-interacting (pressureless).
- Large number of particles. Each class can be described as a continuum (Eulerian approach)

All these assumptions are valid for volcanic ash when you are sufficiently higher than the vent and the deposition layer.

Multiphase flow model: main assumptions

- Discrete number of particle classes (polydispersed grain size)

Total grain size of Vesuvius AD 79 (Pompei) eruption ($d = 2^{-\phi}$ mm)

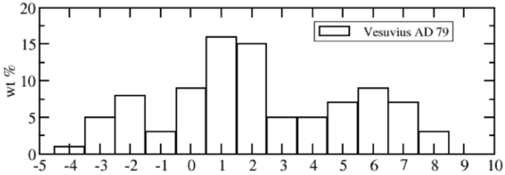

- Heavy particles: $\frac{\hat{\rho}_s}{\hat{\rho}_g} \gg 1$ ($\hat{\rho}_s \approx 400 - 3000$ kg/m^3). Two-way coupling.
- Low concentration $V_s/V := \epsilon_s < 10^{-3}$. Particles are non-interacting (pressureless).
- Large number of particles. Each class can be described as a continuum (Eulerian approach)

All these assumptions are valid for volcanic ash when you are sufficiently higher than the vent and the deposition layer.

Multiphase flow model: main assumptions

- Discrete number of particle classes (polydispersed grain size)

Total grain size of Vesuvius AD 79 (Pompei) eruption ($d = 2^{-\phi}$ mm)

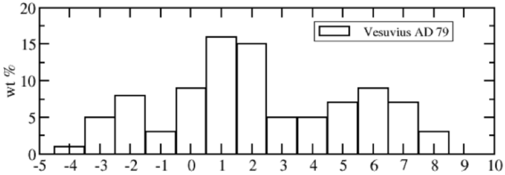

- Heavy particles: $\frac{\hat{\rho}_s}{\hat{\rho}_g} \gg 1$ ($\hat{\rho}_s \approx 400 - 3000$ kg/m^3). Two-way coupling.
- Low concentration $V_s/V := \epsilon_s < 10^{-3}$. Particles are non-interacting (pressureless).
- Large number of particles. Each class can be described as a continuum (Eulerian approach)

All these assumptions are valid for volcanic ash when you are sufficiently higher than the vent and the deposition layer.

Kinematic disequilibrium between particles and carrier fluid

- For relative Reynolds number, $\frac{\rho_g|\mathbf{u}_s-\mathbf{u}_g|d}{\mu} < 1000$, the Stokes law is valid: $\mathbf{f}_d = \frac{\rho_s}{\tau_s}(\mathbf{u}_s - \mathbf{u}_g)$, where the Stokes time is: $\tau_s = \frac{\hat{\rho}_s d_s^2}{18\mu\phi}$ and the empirical correction $\phi = 1 + 0.15\mathrm{Re}_r^{0.687}$
- In turbulent flows, the time scale is $\tau_\eta = \frac{\eta^2}{\nu}$, thus the Stokes number is $\mathrm{St} \equiv \frac{\tau_s}{\tau_\eta} = \frac{\hat{\rho}_s}{18\phi\hat{\rho}_g}(\frac{d_s}{\eta})^2$
- A LES method with grid scale $\xi > \eta$ widens the applicability of the Eulerian approach: $\mathrm{St}_{\mathrm{LES}} = \frac{\hat{\rho}_s}{18\phi\hat{\rho}_g}(\frac{d_s}{\xi})^2(\frac{\xi}{\eta})^{4/3}$
- The gas-particles thermal equilibrium characteristic time is $\tau_T = \frac{\hat{\rho}_s C_{v,s} d_s^2}{4k_s}$, so that $\frac{\tau_T}{\tau_s} = \frac{3}{2}\frac{C_{v,s}\mu}{k_s} = \frac{3}{2}\mathrm{Pr}_s \simeq 10^{-2}$.

Kinematic disequilibrium between particles and carrier fluid

- For relative Reynolds number, $\frac{\rho_g|\mathbf{u}_s-\mathbf{u}_g|d}{\mu} < 1000$, the Stokes law is valid: $\mathbf{f}_d = \frac{\rho_s}{\tau_s}(\mathbf{u}_s - \mathbf{u}_g)$, where the Stokes time is: $\tau_s = \frac{\hat{\rho}_s d_s^2}{18\mu\phi}$ and the empirical correction $\phi = 1 + 0.15\mathrm{Re}_\mathrm{r}^{0.687}$
- In turbulent flows, the time scale is $\tau_\eta = \frac{\eta^2}{\nu}$, thus the Stokes number is $\mathrm{St} \equiv \frac{\tau_s}{\tau_\eta} = \frac{\hat{\rho}_s}{18\phi\hat{\rho}_g}(\frac{d_s}{\eta})^2$
- A LES method with grid scale $\xi > \eta$ widens the applicability of the Eulerian approach: $\mathrm{St}_\mathrm{LES} = \frac{\hat{\rho}_s}{18\phi\hat{\rho}_g}(\frac{d_s}{\xi})^2(\frac{\xi}{\eta})^{4/3}$
- The gas-particles thermal equilibrium characteristic time is $\tau_T = \frac{\hat{\rho}_s C_{v,s} d_s^2}{4k_s}$, so that $\frac{\tau_T}{\tau_s} = \frac{3}{2}\frac{C_{v,s}\mu}{k_s} = \frac{3}{2}\mathrm{Pr}_s \simeq 10^{-2}$.

Kinematic disequilibrium between particles and carrier fluid

- For relative Reynolds number, $\frac{\rho_g|\mathbf{u}_s-\mathbf{u}_g|d}{\mu} < 1000$, the Stokes law is valid: $\mathbf{f}_d = \frac{\rho_s}{\tau_s}(\mathbf{u}_s - \mathbf{u}_g)$, where the Stokes time is: $\tau_s = \frac{\hat{\rho}_s d_s^2}{18\mu\phi}$ and the empirical correction $\phi = 1 + 0.15\mathrm{Re}_r^{0.687}$
- In turbulent flows, the time scale is $\tau_\eta = \frac{\eta^2}{\nu}$, thus the Stokes number is $\mathrm{St} \equiv \frac{\tau_s}{\tau_\eta} = \frac{\hat{\rho}_s}{18\phi\hat{\rho}_g}(\frac{d_s}{\eta})^2$
- A LES method with grid scale $\xi > \eta$ widens the applicability of the Eulerian approach: $\mathrm{St}_{\mathrm{LES}} = \frac{\hat{\rho}_s}{18\phi\hat{\rho}_g}(\frac{d_s}{\xi})^2(\frac{\xi}{\eta})^{4/3}$
- The gas-particles thermal equilibrium characteristic time is $\tau_T = \frac{\hat{\rho}_s C_{v,s} d_s^2}{4k_s}$, so that $\frac{\tau_T}{\tau_s} = \frac{3}{2}\frac{C_{v,s}\mu}{k_s} = \frac{3}{2}\mathrm{Pr}_s \simeq 10^{-2}$.

Kinematic disequilibrium between particles and carrier fluid

- For relative Reynolds number, $\frac{\rho_g|\mathbf{u}_s-\mathbf{u}_g|d}{\mu} < 1000$, the Stokes law is valid: $\mathbf{f}_d = \frac{\rho_s}{\tau_s}(\mathbf{u}_s - \mathbf{u}_g)$, where the Stokes time is: $\tau_s = \frac{\hat{\rho}_s d_s^2}{18\mu\phi}$ and the empirical correction $\phi = 1 + 0.15\mathrm{Re}_r^{0.687}$
- In turbulent flows, the time scale is $\tau_\eta = \frac{\eta^2}{\nu}$, thus the Stokes number is $\mathrm{St} \equiv \frac{\tau_s}{\tau_\eta} = \frac{\hat{\rho}_s}{18\phi\hat{\rho}_g}(\frac{d_s}{\eta})^2$
- A LES method with grid scale $\xi > \eta$ widens the applicability of the Eulerian approach: $\mathrm{St}_{\mathrm{LES}} = \frac{\hat{\rho}_s}{18\phi\hat{\rho}_g}(\frac{d_s}{\xi})^2(\frac{\xi}{\eta})^{4/3}$
- The gas-particles thermal equilibrium characteristic time is $\tau_T = \frac{\hat{\rho}_s C_{v,s} d_s^2}{4k_s}$, so that $\frac{\tau_T}{\tau_s} = \frac{3}{2}\frac{C_{v,s}\mu}{k_s} = \frac{3}{2}\mathrm{Pr}_s \simeq 10^{-2}$.

Dispersed Multiphase Flows: approaches

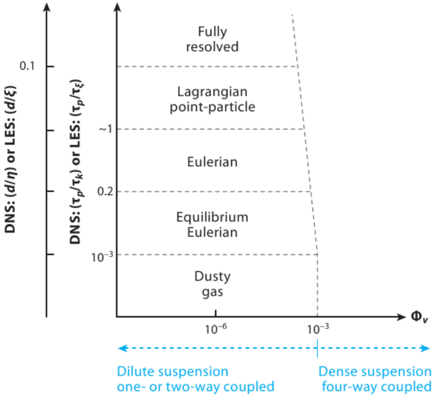

Figure: Approaches to turbulent multiphase flow. Their applicability is separated in terms of time and length scale ratios. *Balachandar & Eaton, 2010*

Dispersed Multiphase Flows: approaches

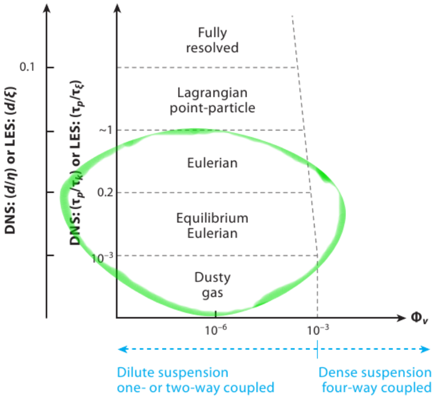

Figure: We focus on the Eulerian case, the Stokes number has to be smaller than 1 and the particle diameter smaller than a threshold.

Polydispersed Eulerian model

$$\partial_t(\rho_i) + \nabla \cdot (\rho_i \mathbf{u}_\mathrm{f}) = 0\,, \quad i = 1 \ldots I \tag{1a}$$

$$\partial_t(\rho_j) + \nabla \cdot (\rho_j \mathbf{u}_j) = 0\,, \quad j = 1 \ldots J \tag{1b}$$

$$\partial_t(\rho_\mathrm{f} \mathbf{u}_\mathrm{f}) + \nabla \cdot (\rho_\mathrm{f} \mathbf{u}_\mathrm{f} \otimes \mathbf{u}_\mathrm{f}) + \nabla p = \nabla \cdot \mathbb{T} + \rho_\mathrm{f} \mathbf{g} - \sum_{j=1}^{J} \mathbf{f}_j \tag{1c}$$

$$\partial_t(\rho_j \mathbf{u}_j) + \nabla \cdot (\rho_j \mathbf{u}_j \otimes \mathbf{u}_j) = \rho_j \mathbf{g} + \mathbf{f}_j\,, \quad j = 1 \ldots J \tag{1d}$$

$$\partial_t(\rho_\mathrm{f} e_\mathrm{f}) + \nabla \cdot (\rho_\mathrm{f} \mathbf{u}_\mathrm{f} e_\mathrm{f}) + p \nabla \cdot \mathbf{u}_\mathrm{f} = \tag{1e}$$

$$= \mathbb{T} : \nabla \mathbf{u}_\mathrm{f} - \nabla \cdot \mathbf{q} + \sum_{j=1}^{J} [(\mathbf{u}_\mathrm{f} - \mathbf{u}_j) \cdot \mathbf{f}_j - Q_j] \tag{1f}$$

$$\partial_t(\rho_j e_j) + \nabla \cdot (\rho_j \mathbf{u}_j e_j) = Q_j\,, \quad j = 1 \ldots J \tag{1g}$$

Constitutive equations

- perfect gas law for the gases (N_2, O_2, H_2O, CO_2, SO_2)
- Constant specific heats for both gas and solid phases
- Sutherland viscosity law for the gases

Particle dynamics in near-equilibrium regime.

Balance of particles momentum.

$$\partial_t \mathbf{u}_s + \mathbf{u}_s \cdot \nabla \mathbf{u}_s = \frac{1}{\tau_s}(\mathbf{u}_g - \mathbf{u}_s) + \mathbf{g}$$

Asymptotic expansion in $1/\tau_s$

Let $\mathbf{a} := \mathrm{D}_t \mathbf{u}_g$ and $\mathbf{w} = \tau_s \mathbf{g}$. Then we find [Ferry & Balachandar (2001)]:

$$\mathbf{u}_s = \mathbf{u}_g + \mathbf{w} - \tau_s(\mathbf{a} + \mathbf{w} \cdot \nabla \mathbf{u}_g) + O(\tau_s^2)$$

- If $a \ll g$, at the first order in τ_s we get $\mathbf{u}_s = \mathbf{u}_g + \mathbf{w}$.
- If $u_g = A\sin(\omega t)$, using the balance equation we find $u_s = \frac{A}{1+\tau_s^2\omega^2}[sin(\omega t) - \tau_s\omega\cos(\omega t)] + u_0 e^{-\frac{t}{\tau_s}}$. On the contrary, using the first order approximation: $u_s = u_g - \tau_s a = A\,[\sin(\omega t) - \tau_s\omega\cos(\omega t)]$.

The equilibrium-Eulerian approximation

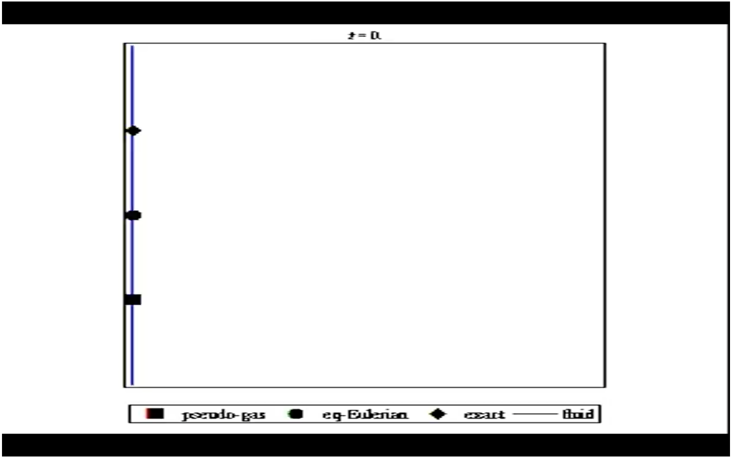

The period is the typical time of this motion. Comparing it with the particles Stokes time, we get $St = 0.2$.

The Equilibrium-Eulerian model

By using the first order approximation of the particle velocity into the Eulerian transport equations, and assuming local thermal equilibrium, we get:

$$\partial_t \beta + \nabla \cdot (\beta \mathbf{u}_\beta) = 0 \tag{2a}$$

$$\partial_t (\beta y_i) + \nabla \cdot (\beta \mathbf{u}_\mathrm{g} y_i) = 0\,, \quad i = 1 \dots I \tag{2b}$$

$$\partial_t (\beta y_j) + \nabla \cdot [\beta (\mathbf{u}_\mathrm{g} + \mathbf{v}_j) y_j] = 0\,, \quad j = 1 \dots J \tag{2c}$$

$$\partial_t (\beta \mathbf{u}_\beta) + \nabla \cdot (\beta \mathbf{u}_\beta \otimes \mathbf{u}_\beta + \beta \mathbb{T}_\mathrm{r}) + \nabla p = \nabla \cdot \mathbb{T} + \beta \mathbf{g} \tag{2d}$$

$$C_\beta [\partial_t (\beta T) + \nabla \cdot (\beta \mathbf{u}_\beta T) + \beta \mathbf{v}_\mathrm{r} \cdot \nabla T] = \\ = -p \nabla \cdot \mathbf{u}_\mathrm{g} + \mathbb{T} : \nabla \mathbf{u}_\mathrm{g} - \nabla \cdot \mathbf{q} - \sum_j \mathbf{v}_j \cdot \mathbf{f}_j\,, \tag{2e}$$

- Equivalent to the Navier-Stokes equations for $(\beta, \mathbf{u}_\beta, T)$ plus some term due to particle decoupling, coupled with a particle transport equation. $\mathbf{u}_\beta = \mathbf{u}_\mathrm{g} + \sum_j y_j \mathbf{v}_j$
- The speed of sound turns out to be $c_\mathrm{DG} = \sqrt{\gamma_\beta p / \beta}$, with $\gamma_\beta = 1 + (\sum_i R_i y_i)/(\sum_i C_i y_i + \sum_j C_j y_j)$

Advantages of the Equilibrium-Eulerian model

- The contribution of the particle inertia can be accurately taken into account by using standard Navier-Stokes numerical algorithm, without needing to implicitly solve the drag term $\mathbf{f}_j$
- Particle decoupling and preferential concentration well modelled up to St $\simeq$ 0.2, keeping the advantages of the Dusty Gas model
- Total number of equation highly reduced for a polydispersed mixture. Eulerian: $I + 3 + 5J$; Equilibrium-Eulerian: $I + 3 + J$.
- Allows to solve efficiently the multiphase dynamics at geophysical scale for particles of size up to $\simeq$ 1 mm.

Non-equilibrium effects in turbulent flows

Preferential Concentration (Equilibrium-Eulerian). $\mathrm{St} = 0.2$.

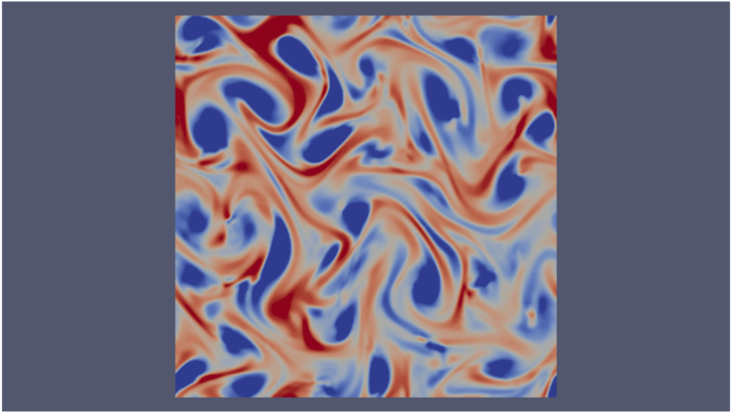

The equilibriumEulerianFoam solver algorithm

We modified the compressible monophase PISO-PIMPLE algorithm

- predictor for the mixture density β
- solve for the mass fractions $y_{i,j}$
- predictor for the mixture velocity $\mathbf{u}_\beta$
- solve for the mixture temperature T
- corrector loop
  - find correction to solid phases velocity $\mathbf{v}_j$ based on acceleration
  - solve for pressure p
  - correct velocity and fluxes
- correct mixture density

Large Eddy Simulation models

We implemented the following LES models for the subgrid terms of the compressible equilibrium-Eulerian model:

- Compressible Smagorinsky (static and dynamic)
- Moin model (dynamic)
- TKE model (static and dynamic)
- WALE model (static and dynamic)

Numerical benchmark: compressible, homogeneous and isotropic turbulence

Decaying turbulence with initial kinetic energy spectrum:

$E(k) \propto \left(\frac{k}{k_0}\right)^4 \exp\left(-2\left(\frac{k}{k_0}\right)^2\right)$. Here k is the eddy wavenumber.

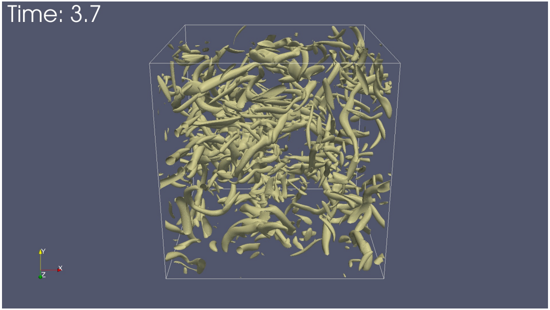

Compressible homogeneous and isotropic turbulence with $\mathrm{Ma}_{\mathrm{rms}} = 0.2$, compressibility factor $\chi_0 = 0$ and $\mathrm{Re}_\lambda = 116$, in a box with 256^3 cells.

Numerical benchmark: compressible, homogeneous and isotropic turbulence

The solver is able to simulate accurately the turbulence.

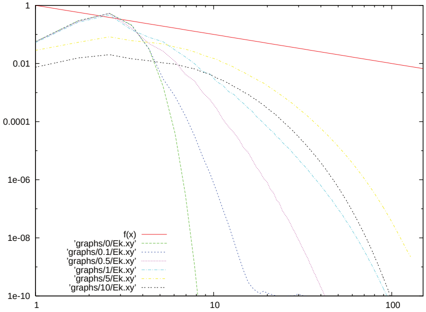

(a) Evolution of the turbulent kinetic energy spectrum. The straight line is the $k^{-5/3}$ behavior predicted by Kolmogorov.

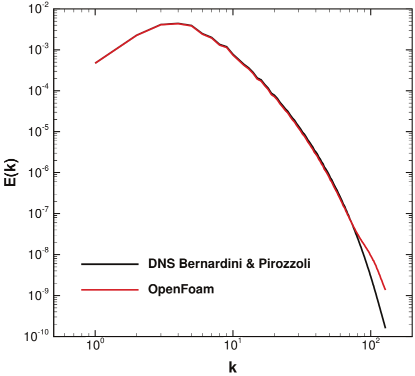

(b) Test case validation: comparison with an eight order DNS after one large-eddy turnover time (10000 time steps).

Numerical benchmark: compressible, homogeneous and isotropic turbulence

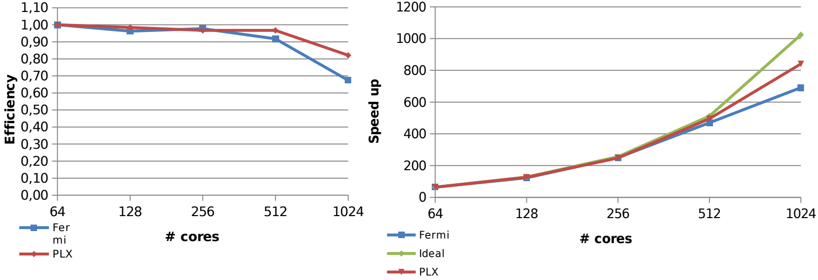

Figure: Scalability test on PLX and FERMI environments (with little output work). Collaboration between us and *Paride Dagna*.

In order to fix ideas, the solver reach a velocity in the range 1÷10 Mcells/s on 1024 cores (multiphase÷monophase) .

LES vs DNS

Static — Dynamic

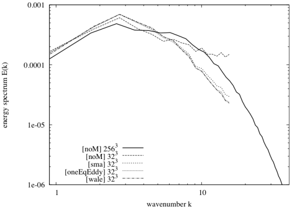

(a) $\mathcal{E}(k)$ at $t/\tau_e = 5.465$

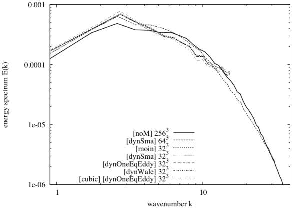

(b) $\mathcal{E}(k)$ at $t/\tau_e = 5.465$

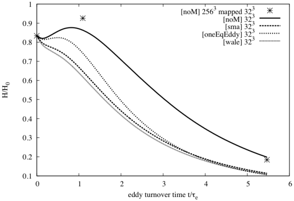

(c) Evolution of $\mathcal{H}/\mathcal{H}_0$

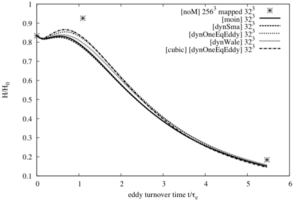

(d) Evolution of $\mathcal{H}/\mathcal{H}_0$

LES vs DNS

Static — Dynamic

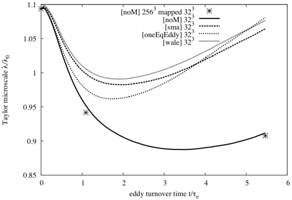

(e) Evolution of $\lambda_{\mathrm{T}}/\lambda_{\mathrm{T},0}$

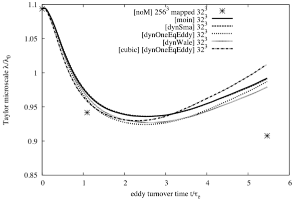

(f) Evolution of $\lambda_{\mathrm{T}}/\lambda_{\mathrm{T},0}$

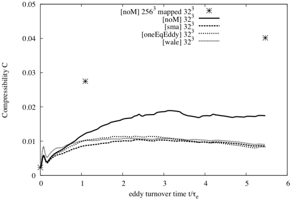

(g) Evolution of $\mathcal{C}$

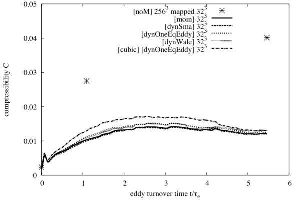

(h) Evolution of $\mathcal{C}$

Heat transfer

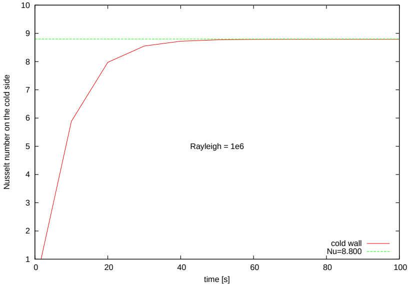

Natural convection/heat transfer in a square cavity with the top and bottom walls insulated and the left (hot) and right (cold) walls with a fixed temperature.

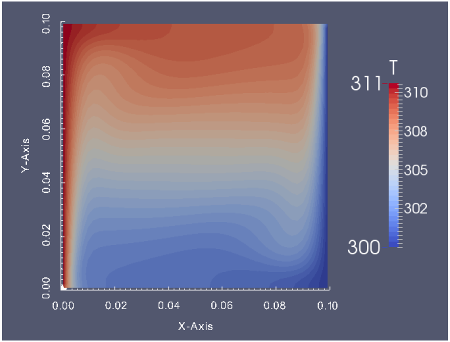

The reference value Nu $=$ 8.800 is taken from V.A.F. Costa, Double diffusive natural convection in a square enclosure with heat and mass diffusive walls, *Int. J. Heat Mass Transfer*, 40 (1997) 4061–4071.

Experimental forced plume

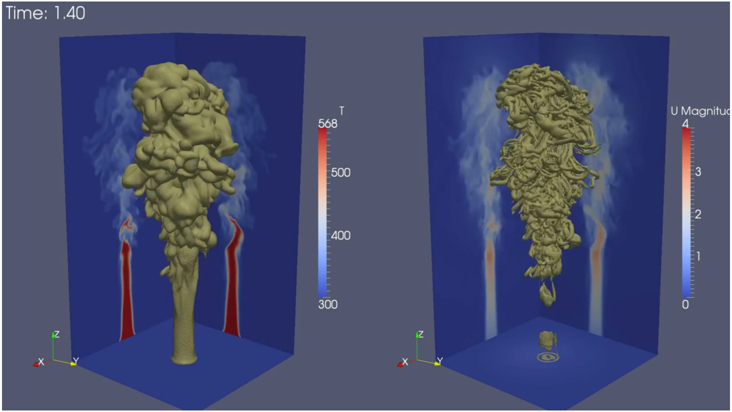

Experimental plume (domain height 1.14 m) with initial momentum and buoyancy. 11 Mcells. Re $\simeq$ 2000. The inlet boundary condition has been implemented in order to take into account the mean inlet velocity shape, turbulent fluctuations and forcing.

Pyroclastic density currents benchmark

Geometry

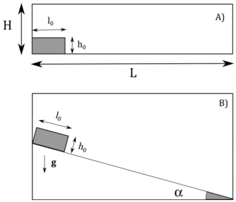

2D Cartesian domain (L×H)
(in 3D assume symmetric initial conditions)
L=10 km
H=1 km
(non-dimensionalization is possible)

α = 15 deg ($\pi/12$ rad)
Aspect ratio AR=h_0/l_0=0.8

Initial conditions

Dilute current

Volume (A=$h_0 \times l_0$)	200000 m^2
Volumetric particle concentration (Φ_0)	**5×10^{-4}**
Solid bulk density	1 kg/m^3
Total mass (*)	2×10^5 kg/m
Gravity acceleration	-9.81 m/s^2
Grain size (spherical)	125 μm
Particle density	2000 kg/m^3
Temperature	300 K / 500 K
Geometry	A) B)

Pyroclastic density currents benchmark

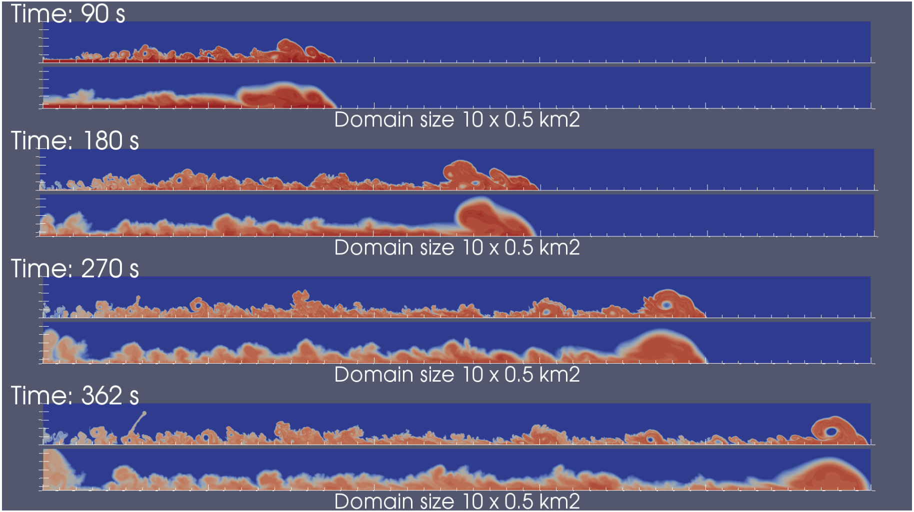

Resolution 1 m vs 10 m with the dynamic WALE LES model (5 Mcells vs 50 kCells)

Pyroclastic density current benchmark

Starting from this simple case, we are studying the effect of:

- turbulent mixing
- subgrid model
- 3D vs 2D
- obstacles
- slope
- topography
- polydispersity of the mixture (up to 10 particle classes)
- dense deposit layer (comparing with other codes)

Volcanic plumes

We are participating to an international benchmark initiative involving two numerical simulations:

weakPlume

- duration: 0.2 hours
- Mass flow rate: $1.5 * 10^6$ kg/s
- Exit velocity: 135 m/s
- Exit temperature: 1273 K
- Exit gas fraction: 3 wt%
- Grain size distribution:
  - coarse: 1 mm
  - fine: 62.5 μm

strongPlume

- duration: 2.5 hours
- Mass flow rate: $1.5 * 10^9$ kg/s
- Exit velocity: 275 m/s
- Exit temperature: 1053 K
- Exit gas fraction: 5 wt%
- Grain size distribution:
  - coarse: 0.5 mm
  - fine: 15.6 μm

weakPlume – dynamic WALE – 200 kCells

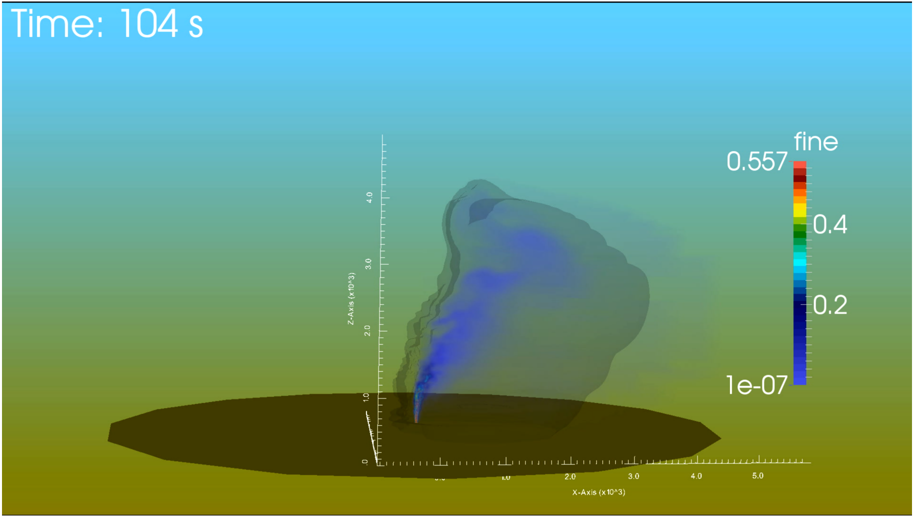

strongPlume – dynamic WALE – 8 Mcells

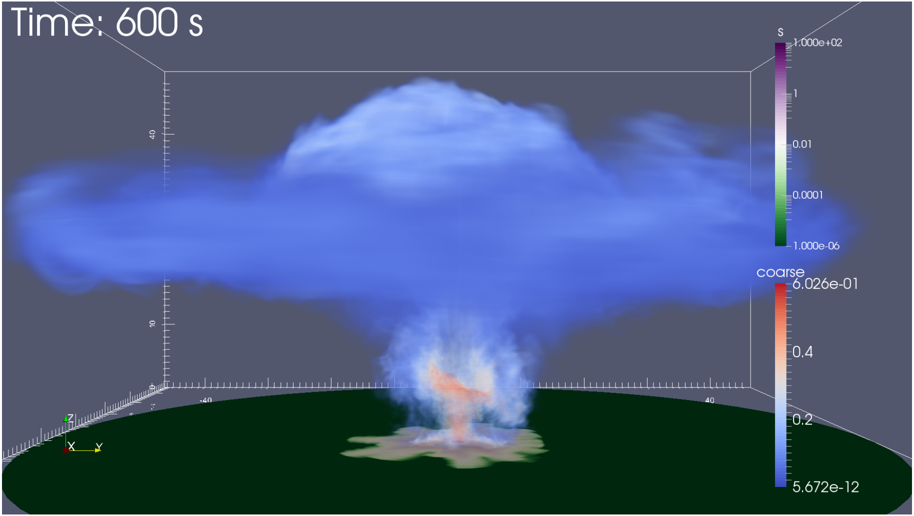

strongPlume – dynamic WALE – 8 Mcells

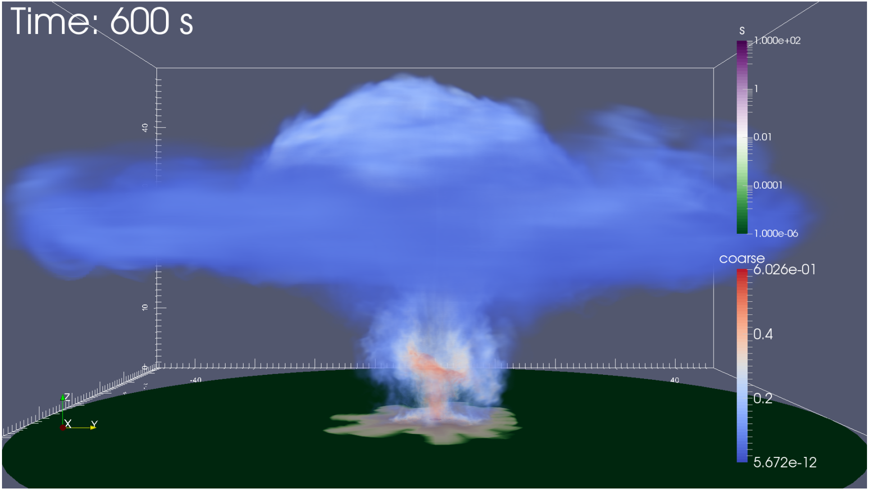

Figure: 1 mm ash mass fraction and total deposit thickness.

strongPlume – dynamic WALE – 8 Mcells

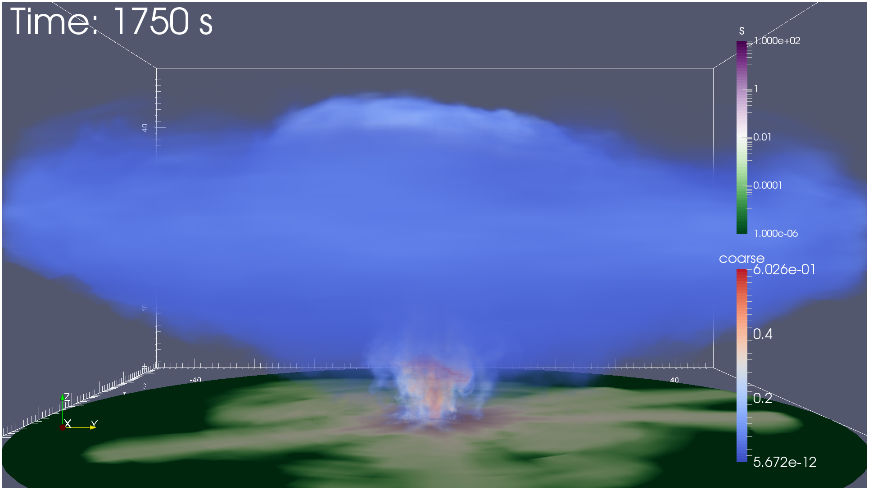

Figure: 1 mm ash mass fraction and total deposit thickness.

strongPlume – dynamic WALE – 8 Mcells

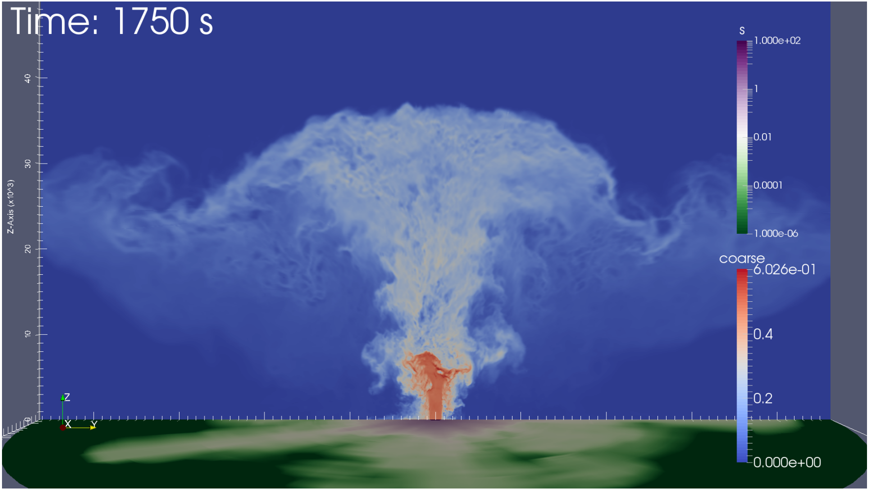

Figure: 1 mm ash mass fraction and total deposit thickness.

strongPlume – dynamic WALE – 8 Mcells

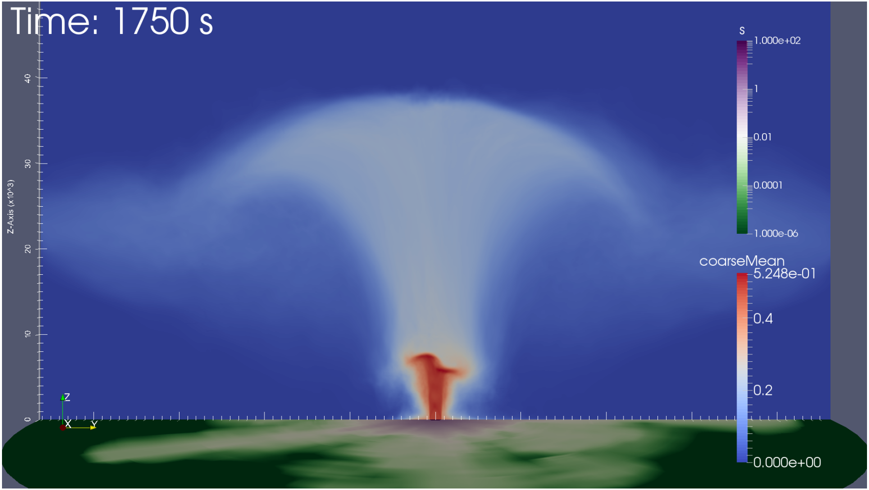

Figure: 1 mm ash mean mass fraction and total deposit thickness.

strongPlume – dynamic WALE – 8 Mcells

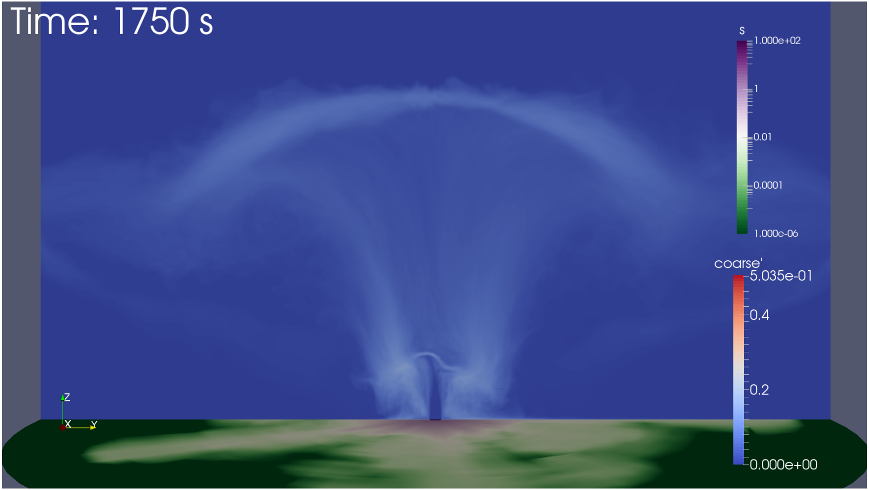

Figure: 1 mm ash mass fraction fluctuations and total deposit thickness.

strongPlume – dynamic WALE – 8 Mcells

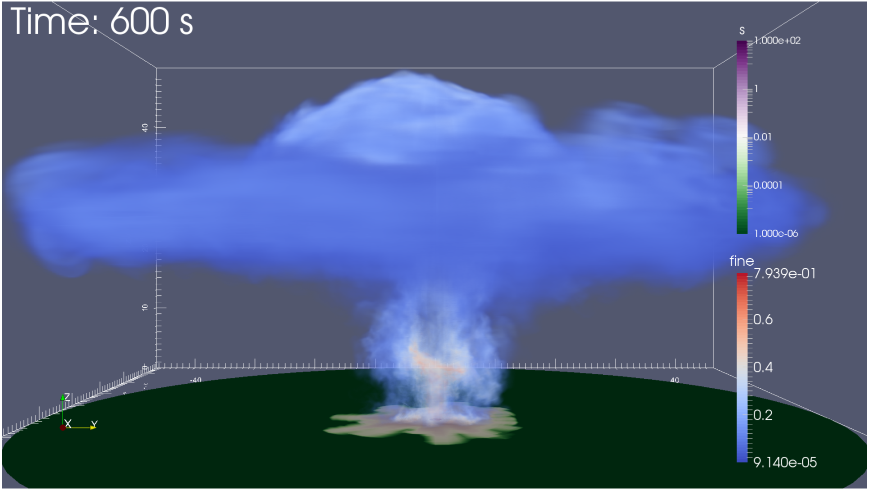

Figure: 15.6 μm ash mass fraction and total deposit thickness.

strongPlume – dynamic WALE – 8 Mcells

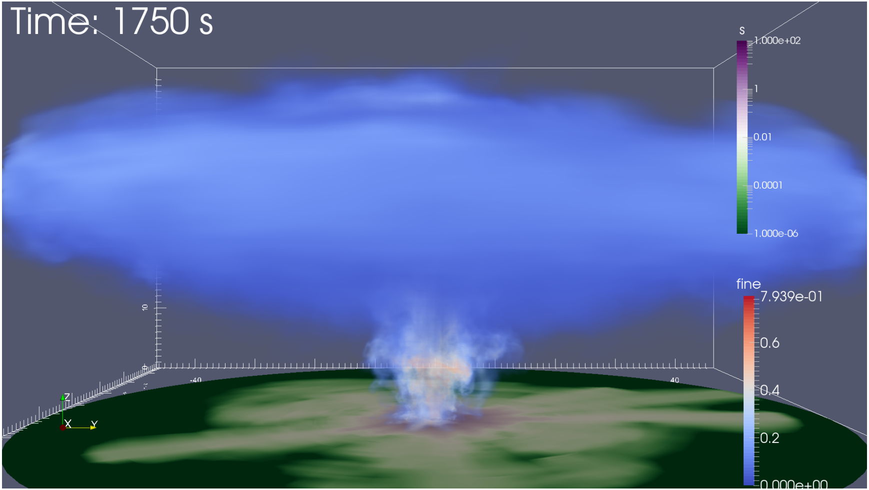

Figure: 15.6 μm ash mass fraction and total deposit thickness.

strongPlume – dynamic WALE – 8 Mcells

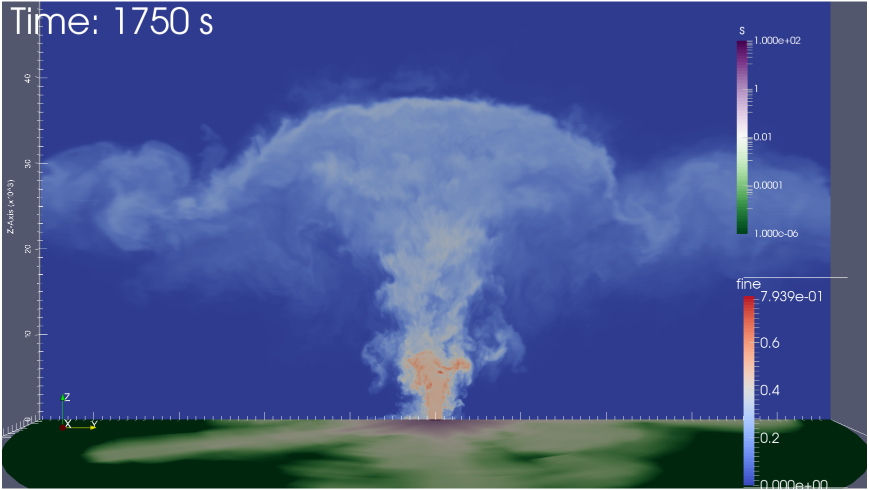

Figure: 15.6 μm ash mass fraction and total deposit thickness.

strongPlume – dynamic WALE – 8 Mcells

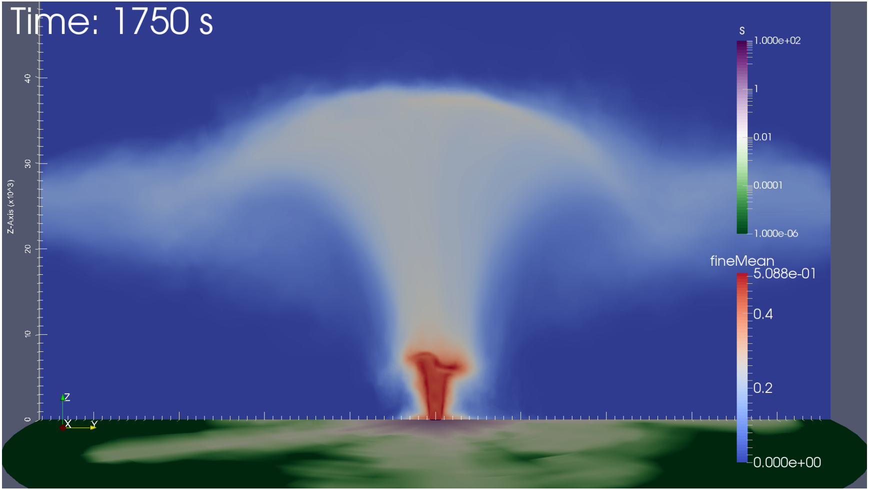

Figure: 15.6 μm ash mean mass fraction and total deposit thickness.

strongPlume – dynamic WALE – 8 Mcells

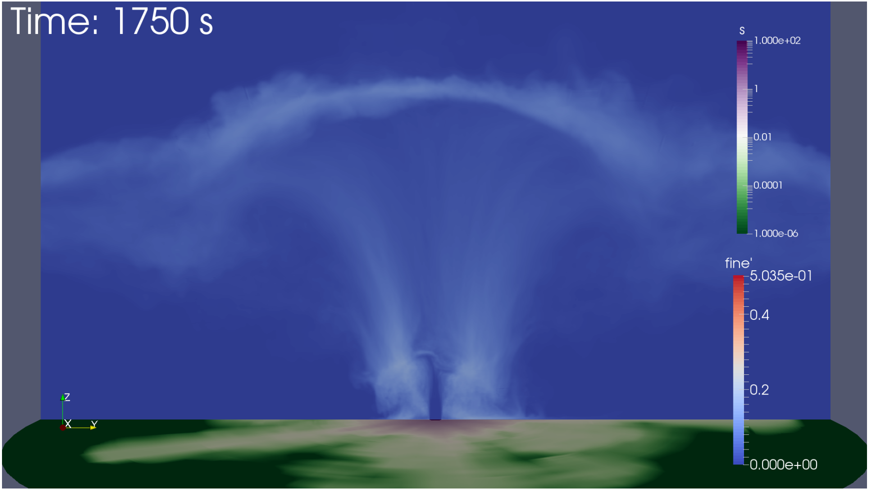

Figure: 15.6 μm ash mass fraction fluctuations and total deposit thickness.

strongPlume – dynamic WALE – 8 Mcells

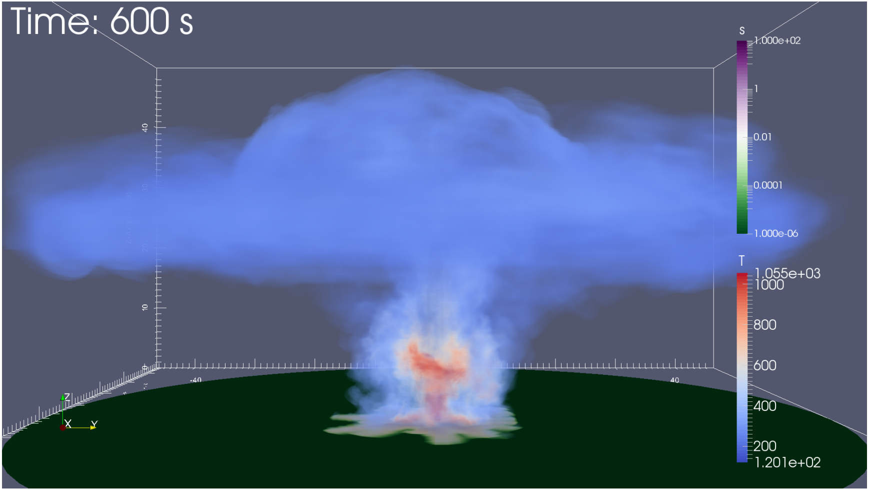

Figure: Temperature and total deposit thickness.

strongPlume – dynamic WALE – 8 Mcells

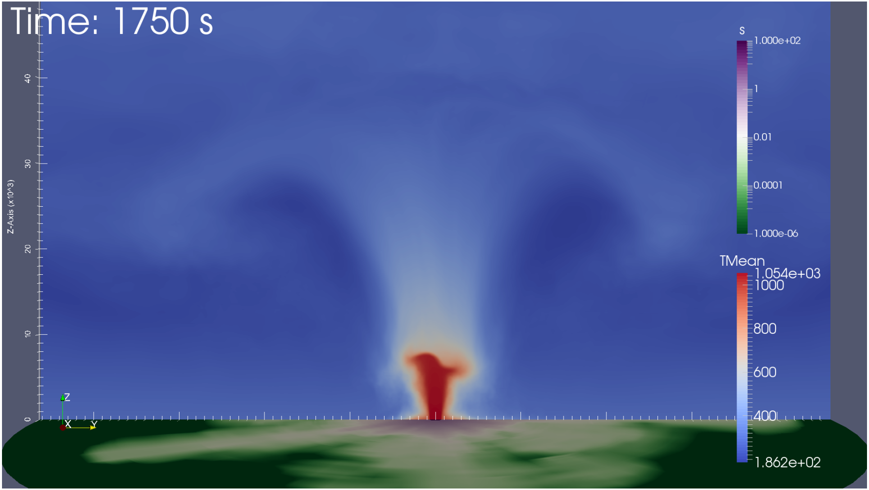

Figure: Mean temperature and total deposit thickness.

strongPlume – dynamic WALE – 8 Mcells

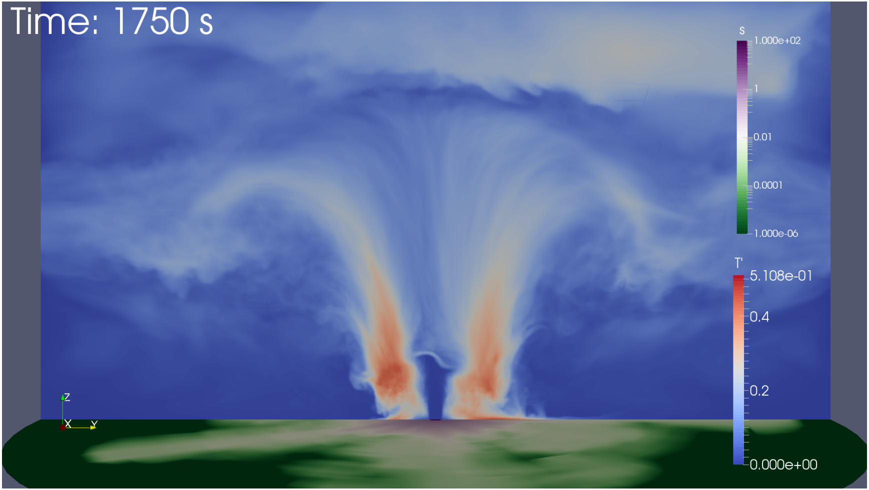

Figure: Temperature fluctuations and total deposit thickness.

strongPlume – dynamic WALE – 8 Mcells

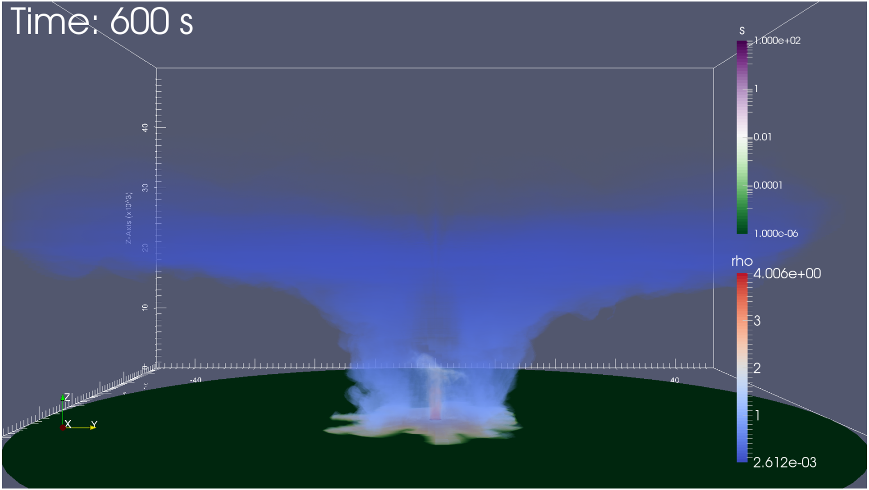

Figure: Mixture density and total deposit thickness.

strongPlume – dynamic WALE – 8 Mcells

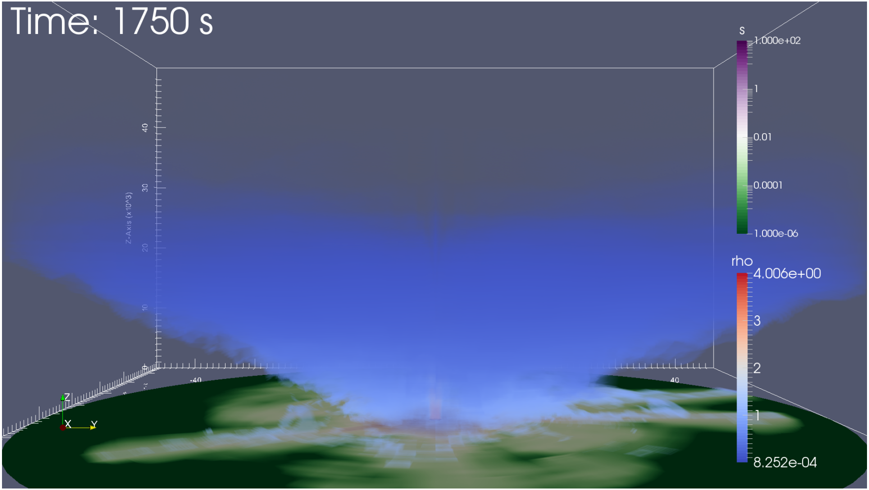

Figure: Mixture density and total deposit thickness.

strongPlume – dynamic WALE – 8 Mcells

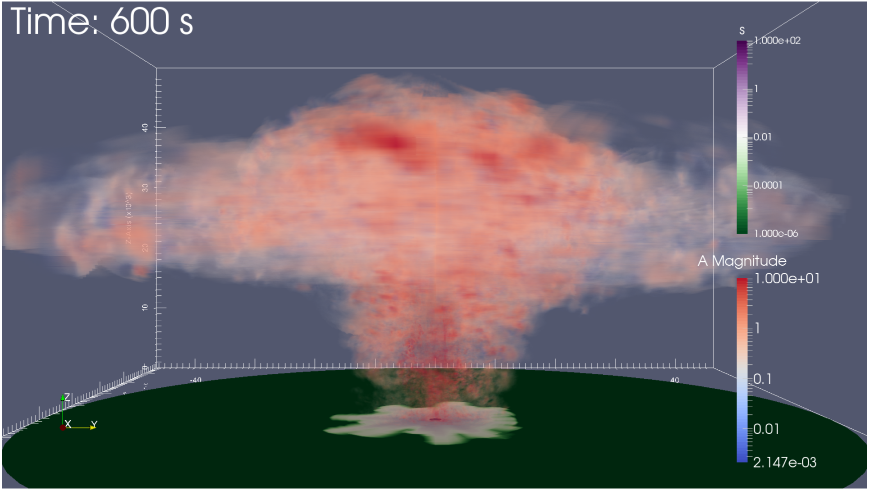

Figure: Acceleration and total deposit thickness.

strongPlume – dynamic WALE – 8 Mcells

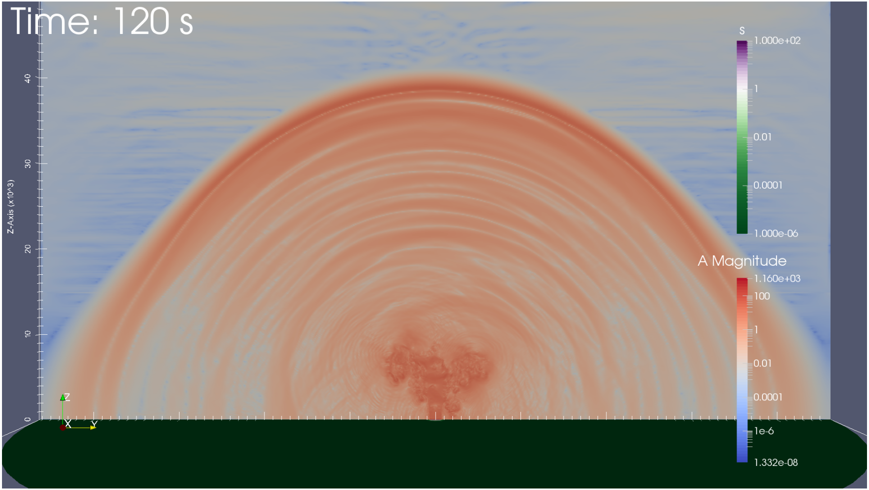

Figure: Acceleration and total deposit thickness.

strongPlume – dynamic WALE – 8 Mcells

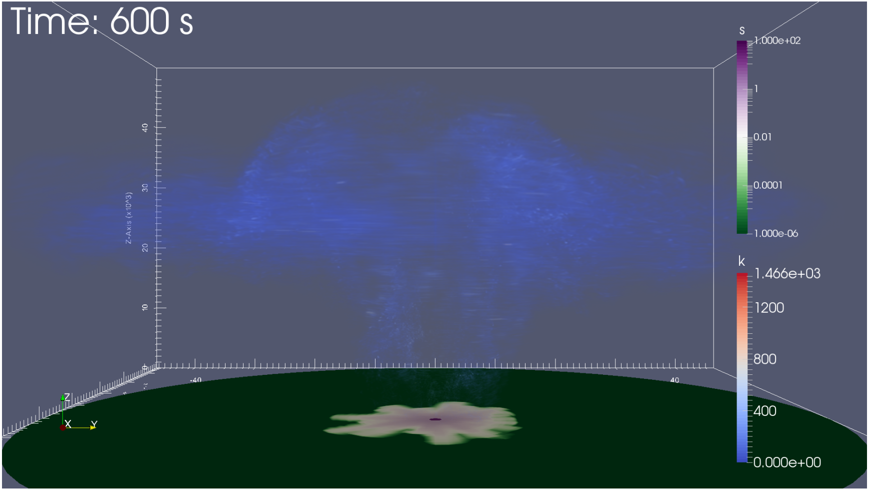

Figure: Subgrid kinetic energy and total deposit thickness.

strongPlume – dynamic WALE – 8 Mcells

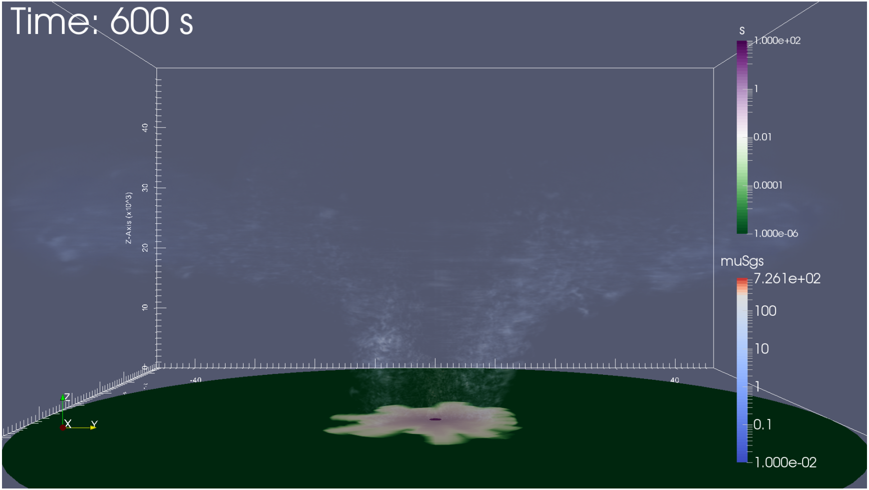

Figure: Turbulent viscosity and total deposit thickness.

strongPlume – dynamic WALE – 8 Mcells

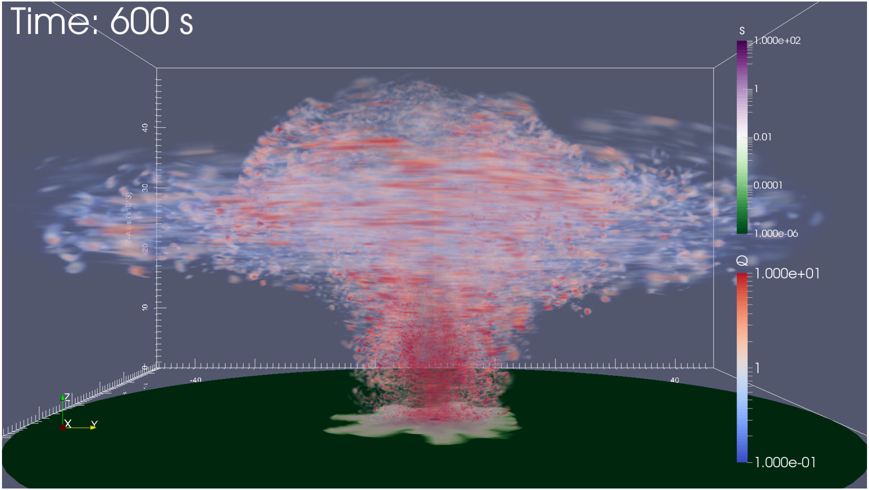

Figure: Second invariant of the velocity gradient Q and total deposit thickness.

Volcanic plume analysis

We are interested in:

- Effect of the subgrid model
- Effect of grid refinement
- Comparison with integral 1D models and other 3D codes
- Entrainment coefficient evolution (key parameter for 1D integral models)
- Effect of decoupling
- Effect of polydispersion
- Effect of wind and humidity
- Deposit evolution
- Interaction between settling particles and entraining air
- Interaction between pyroclastic density currents and the plume
- Infrasound generation

Future work

- Construct a good mesh in presence of wind
- Include topography
- Include particle aggregation
- Include water condensation
- Implement non-reflecting boundary conditions
- Increment the number of cores and cells

Conclusions

- We have developed the compressible version of the equilibrium-Eulerian model (two-way coupling)
- We have implemented it into the OpenFOAM infrastructure
- The new solver is able to accurately and efficiently capture clustering, preferential concentration and settling up to 1 mm particles
- the solver has been tested up to 1024 cores. It shows a good efficiency ($> 60\%$) on the Cineca Fermi infrastructure

Thank You!

Contacts

- email: *matteo.cerminara@ingv.it*
- research web-page: *https://sites.google.com/site/matteocerminara*
- CFD movies: *https://www.youtube.com/user/MatteoCerminara*